Structural Characterization of Various Chiral Smectic-*C* Phases by Resonant X-Ray Scattering

P. Mach,[1] R. Pindak,[2] A.-M. Levelut,[3] P. Barois,[4] H. T. Nguyen,[4] C. C. Huang,[1] and L. Furenlid[5]
[1]*School of Physics and Astronomy, University of Minnesota, Minneapolis, Minnesota 55455*
[2]*Bell Laboratories, Lucent Technologies, Murray Hill, New Jersey 07974*
[3]*Laboratoire de Physique des Solides, Univ. Paris-Sud, F-91405 Orsay, France*
[4]*Centre de Recherche Paul Pascal, CNRS, Univ. Bordeaux I, Avenue A. Schweitzer, F-33600 Pessac, France*
[5]*NSLS, Brookhaven National Laboratory, Upton, New York 11973*
(Received 12 May 1998)

We report the results of resonant x-ray diffraction at the sulfur K-edge performed upon free-standing films of a thiobenzoate liquid-crystal compound. Our data provide the first direct structural evidence of distinct periodicities in several chiral Sm-C phases, including 2-layer, 3-layer, and 4-layer superlattices in Sm-C_A^*, Sm-C_{FI1}^*, and Sm-C_{FI2}^*, respectively. In Sm-C_α^*, periodicity incommensurate with the layer spacing was detected. The racemic compound version was also studied. The results are consistent with a "clock model" of the Sm-C^* variant structures. [S0031-9007(98)06747-7]

PACS numbers: 61.30.Eb

The recent discovery of the chiral antiferroelectric smectic-C phase (Sm-C_A^*) in a liquid-crystal compound [1] showed that interlayer antiferroelectric ordering can be stabilized in a mesophase *without long-ranged positional order*. This surprising and fundamental condensed matter finding prompted intensive research into the structure of Sm-C_A^*. A consequence of this effort has been the identification of several other chiral Sm-C (Sm-C^*) variants [2]. These novel phases include the so-called Sm-C_{FI1}^* and Sm-C_{FI2}^*, which exhibit ferrielectric behavior, and the Sm-C_α^*. Detailed experimental studies of these phases, followed by development of a theoretical model describing the relevant intermolecular interactions which drive the Sm-C_α^*-Sm-C^*-Sm-C_{FI2}^*-Sm-C_{FI1}^*-Sm-C_A^* transition sequence, remain an important fundamental research goal. Moreover, the distinct electro-optic responses of the subphases, especially Sm-C_A^*, are of applied interest, having already been employed in fast optical switching devices with tristable properties [3].

A variety of experimental probes has been used to obtain information about Sm-C_A^* and associated phases, including x-ray diffraction [4–6], calorimetric investigations [7,8], electro-optic response studies [2,7], and optical measurements [9]. Unfortunately, these studies have generally not been able to provide detailed information about the molecular arrangements of most of these phases [10]. Because many different models have been proposed for the Sm-C^* variant structures [2,4,11–14], the ability to discriminate experimentally the actual molecular arrangements is critically important. Conventional x-ray diffraction, normally a powerful tool for resolving such issues, is unable to supply the necessary information, for reasons discussed below. In this Letter, we report the application of resonant x-ray diffraction to studying molecular structures of four Sm-C^* variant phases found in (R)-enantiomer and racemic versions of one compound. Our results yield the first direct structural observation of distinct superlattice periodicities associated with the Sm-C_A^*, Sm-C_{FI1}^*, Sm-C_{FI2}^*, and Sm-C_α^* phase series. The results enable us to discriminate among several theoretical models.

In the smectic phases, the elongated liquid-crystal molecules order to give a layered center-of-mass distribution. Within each molecular layer, the positional order is liquid-like, but definite orientational order exists. The molecules' long axes align along a common direction, the so-called director **n**. The director is either along the layer normal **n** (Sm-A phase), or is inclined with respect to **z** by some tilt angle θ (Sm-C^* phases). Within the Sm-C^* phases, a projection (**c**) of the molecular director **n** onto the layer plane can be considered. The situation is shown in Fig. 1. The angle between **c** and the x axis

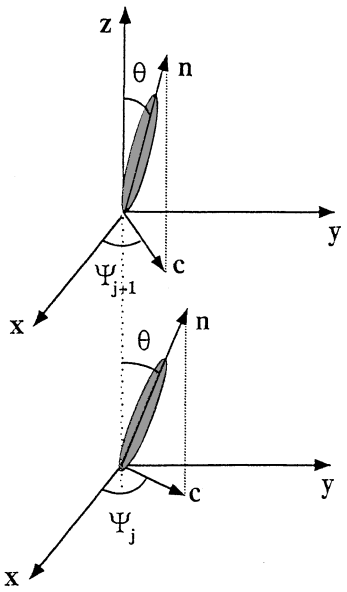

FIG. 1. Schematic diagram illustrating the orientation of molecules in neighboring Sm-C^* layers. Tilt angle θ in layers j and $j+1$ is the same, while azimuthal angles Ψ_j and Ψ_{j+1} differ. **z**, **n**, and **c** are coplanar.

in the jth layer is denoted as Ψ_j, and the change in Ψ_j between adjacent layers j and $(j + 1)$ as $\Delta\Psi_j$. It is in the detailed progression of Ψ_j and $\Delta\Psi_j$ from layer to layer where proposed models of the molecular arrangements in the Sm-C^* variants differ. Molecular chirality induces a further helical rotation of **c** about the z axis. The pitch P_0 of this helix is usually in the optical wavelength range. P_0 is therefore much greater that the characteristic $\Delta\Psi_j$ periodicities which we have observed, as discussed in this Letter.

Many liquid crystals in the smectic phase can be spread as free-standing films. In the case of these substrate-free films, the layer and film normals coincide, and the film thickness is quantized to a discrete number of layers. In practice, uniform films ranging from two to hundreds of layers in thickness are easily prepared. The liquid-crystal compound in our experiment was studied in such a free-standing film geometry, thereby providing a well-defined, uniform orientation of the smectic layers with respect to the incident x-ray beam without the need for any aligning surface that would attenuate the x-ray intensity. The x-rays were incident onto the film in the Bragg geometry.

The material studied in our experiment is the $n = 10$ member (hereafter referred to as 10OTBBB1M7) of the homologous series whose molecular structure is given in Fig. 2. Physical properties of selected compounds from this series have been published elsewhere [7]. The bulk 10OTBBB1M7 enantiomer shows the following phase sequence: Isotropic (152.6 °C) Sm-A (123.6 °C) Sm-C^*_α (120.2 °C) Sm-C^* (119.2 °C) Sm-C^*_{FI2} (114 °C) Sm-C^*_{FI1} (112 °C) Sm-C^*_A (109.7 °C) crystal. A critical feature of the 10OTBBB1M7 material for the purposes of our experiment is the sulfur atom contained within the rigid, center portion of the molecule. Conventional x-ray diffraction along the Q_z reciprocal space direction probes the in-plane-averaged electron density. All of the SmC^* variants give Q_z peaks only at integral multiples of $Q_0 = 2\pi/d$, where d is the smectic layer spacing. Therefore, the z-projected electron density is identical for all of the variants, and they differ from one another only by symmetry elements such as glide planes or screw axes along **z**. By working with x-rays whose energy is at the sulfur's K absorption edge, the structure factor becomes a tensor instead of the conventional scalar [15]. The scattered x-ray intensity now varies depending on the molecular orientation, since the off-diagonal tensor components depend on the orientation of the bonds around the sulfur atom with respect to the polarization of the incident x-ray beam [16]. Because $\Delta\Psi_j$ arrangements of various Sm-C^* subphases are distinct, under this circumstance the resonant x-ray diffraction is capable of revealing the structural differences.

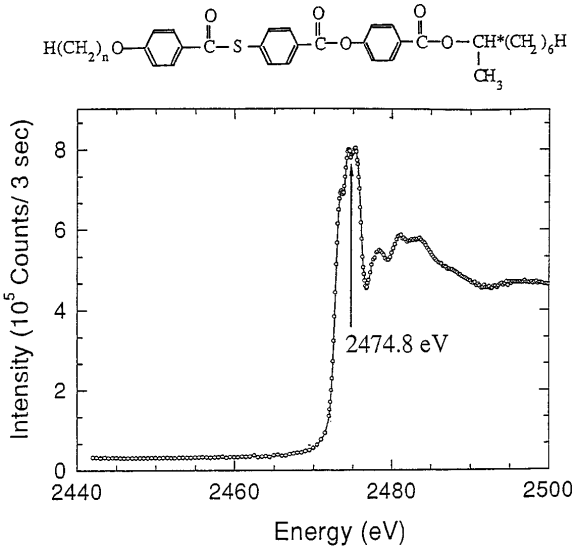

FIG. 2. Fluorescence intensity versus x-ray beam energy incident onto bulk 10OTBBB1M7 powder sample. Shown above is the homologous series of which 10OTBBB1M7 is the $n = 10$ member.

The x-ray data reported here were obtained at beamline X-19A of the National Synchrotron Light Source. Free-standing films of 10OTBBB1M7 material, 1 cm in diameter and approximately 250 layers thick, were prepared inside a temperature-controlled oven. Windows above the film allowed for optical access, enabling us to monitor film thickness and uniformity. Apertures in the side walls allowed the x-rays to enter and exit the oven. The entire x-ray path between beamline vacuum and the x-ray detector was slowly flushed with helium to avoid air absorption of the approximately 2.5 keV x-ray beam; the choice of beam energy was dictated by the need to match the sulfur's K absorption edge. The FWHM of our system resolution function was $\Delta Q_Z = 3.5 \times 10^{-3} Q_0$. Also, the upstream flight path ahead of the oven allowed for insertion of powder 10OTBBB1M7 into the direct beam, with a fluorescence detector mounted at 90° to the x-ray path. As shown in Fig. 2, this enabled us to measure the sulfur K-edge absorption peaks for 10OTBBB1M7 by monitoring the fluorescence intensity as a function of incident beam energy. The principal maximum, E_0, occurs at 2475 eV.

With the x-ray energy tuned to E_0, Q_z/Q_0 scans were performed at a sequence of temperatures. Representative diffracted intensity scans for several 10OTBBB1M7 phases are displayed in Fig. 3; the top four curves are for the (R) enantiomer, while the bottom data set was taken from a 10OTBBB1M7 racemic film of comparable thickness [17]. All of the Sm-C^* variants clearly exhibit non-integral peaks of resonant scattering origin, including, for instance, satellite peaks about Q_0 and $2Q_0$ in the Sm-C^*_α phase. At temperatures within the Sm-C^*_{FI2} phase, shown in Fig. 3(b), satellite peaks are located at $1.25Q_0$, $1.5Q_0$, $1.75Q_0$, and $2.25Q_0$. These quarter-integer peaks indicate a 4-layer superlattice periodicity along the smectic layer normal direction. In the Sm-C^*_{FI1} phase [Fig. 3(c)], one-third integer peaks are evident, implying a three-layer

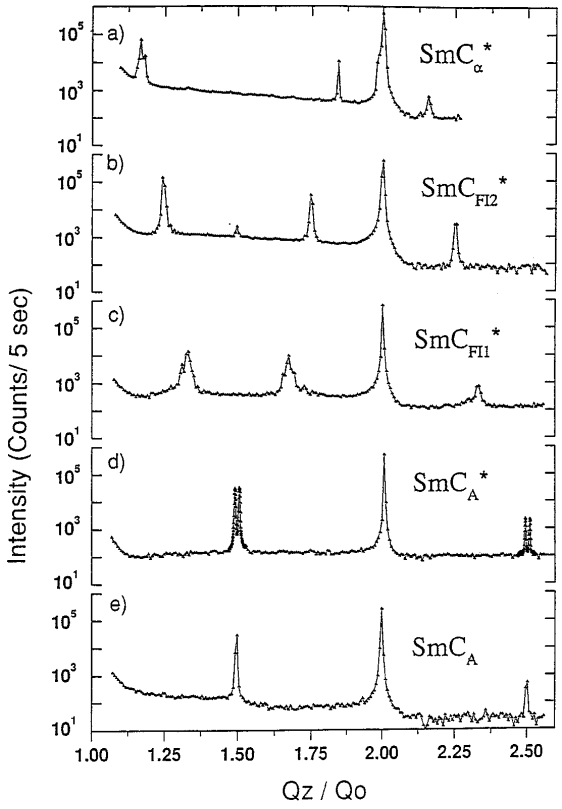

FIG. 3. X-ray intensity scans in the indicated phases of (R)-enantiomer (plots a-d) and racemic 10OTBBB1M7 (plot e). The temperatures corresponding to curves ($a-e$) are 119.0, 115.4, 113.2, 109.3, and 107.0 °C, respectively.

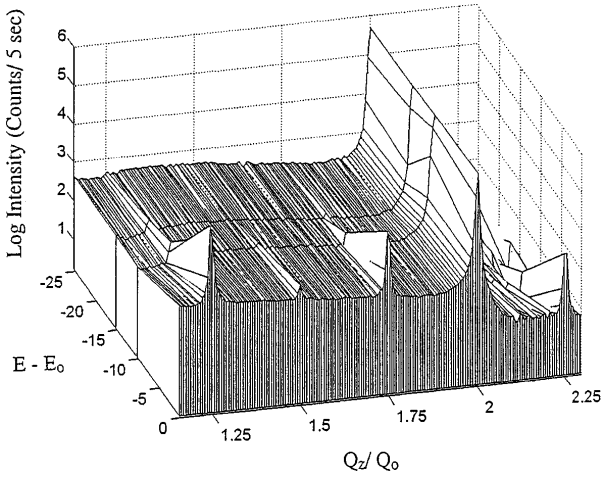

FIG. 4. X-ray intensity scans in the Sm-C^*_{FI2} phase of the 10OTBBB1M7 (R)-enantiomer as a function of incident beam energy relative to the sulfur K-edge absorption maximum.

superlattice periodicity. Within the Sm-C^*_A phase and Sm-C_A phases [Figs. 3(d) and 3(e)], peaks very close to (or even at) half-integer Q_z/Q_0 values correspond to a nearly two-layer superlattice. These data represent to our knowledge the first direct structural observation of characteristic superlattice periodicities associated with the various antiferro- and ferrielectric Sm-C^* liquid-crystal subphases [10]. The resonant peaks are approximately resolution-limited, except for the one-third order peaks, which are significantly broader, indicating a more disordered structure, or perhaps unresolved subfeatures. The importance of performing the measurements at the sulfur absorption peak, E_0, is illustrated in Fig. 4, which shows a series of scans taken in the Sm-C^*_{FI2} phase. Similar scans were made for each of the nonintegral peaks in the various phases; in all cases, the peaks vanished for $|E - E_0| > 25$ eV, confirming their resonant scattering origin.

The models which have been proposed to describe the Sm-C^* variants can be distinguished based on the values of $\Delta\Psi_j$ predicted. In addition to the long helical structure (pitch length of order 1 μm), all of the models predict a repeating series of $\Delta\Psi_j$ values with a Ψ_j periodicity of υ layers. Two models are "Ising- like" in that they predict a $\Delta\Psi_j$ of either 0 or π exclusively, although the "T-Ising" [2,4,11] and "E-Ising" [2,12] models, as we denote them here, predict differing $\Delta\Psi_j$ sequences [18]. What we call the "bilayer" model [13] proposes a two-layer ($\upsilon = 2$) repeating unit, with $\Delta\Psi_j$ taking on alternating values of $+\delta\Psi$ and $-\delta\Psi$. Lastly, a structure has been proposed [14] which we denote here as "clock" model that allows for a constant $\Delta\Psi_j = 2\pi/\upsilon$.

A comparison between the experimental data and structure factor calculations similar to those presented by Dmitrienko [15] allows us to rule out most of the proposed models. The calculations give the resonant scattering component of the structure factor, which is the only component we measured at satellite positions. For instance, the four-layer period T- and E-Ising-like models [18] predict either no resonant component for half-order satellites (T Ising) or an equal intensity for the half- and quarter-order peaks (E Ising). Additionally, the double layer periodicity of the $\Delta\Psi_j$ sequence for T Ising [18] should actually give *conventional* half-order peaks. Since Fig. 3(b) shows both quarter-order and half-order *resonant* peaks, but differing by an order of magnitude in intensity, the Sm-C^*_{FI2} results are inconsistent with these two Ising-like models [19]. Moreover, the "bilayer" model is ruled out by the observation of quarter-order peaks. In fact, if we compare the intensities of the satellite peaks within the different phases, it is only the "clock" model which could consistently describe the whole range of x-ray signatures we observe for the Sm-C^* variants. Using this model, we can also advance an explanation for the suggestive splitting ($\pm 0.008 Q_0$) of the peaks at $Q_z = 1.5Q_0$ and $2.5Q_0$ for the Sm-C^*_A phase of the enantiomer. Structure factor calculations based upon the clock-like evolution of $\Delta\Psi_j$ predict x-ray peaks at $Q_z = lQ_0 + mQ_s$, with integer l, and $m = 0$, ± 1, or ± 2. Here $Q_s = 2\pi(1/\upsilon d + 1/P_0)$ and reflects both the superlattice and optical pitch periodicities in the molecular arrangements. Inserting the measured Sm-C^*_A layer

spacing $d = 38.3$ Å and the observed Q_z splitting for Fig. 3(d) gives $\nu = 2$ as expected and $P_0 = 4800$ Å [20]. The Sm-C_A phase of the racemate notably lacks splitting in its half-integer satellite peaks, consistent with there being no optical pitch term in the appropriate Q_s [21]. Similar analysis of satellite peaks shows incommensurate periodicity (noninteger ν), evolving from roughly eight to five layers with decreasing temperature, in the Sm-C^*_α phase window. A more complete description of these observations will be presented in a future publication.

Summarizing, we have applied resonant x-ray diffraction to study free-standing films of a liquid-crystal compound exhibiting a phase sequence of Sm-C^*_α, Sm-C^*, Sm-C^*_{FI2}, Sm-C^*_{FI1}, and Sm-C^*_A. Our results provide the first direct structural evidence for distinct superlattice periodicities in these Sm-C^* variants. The Sm-C^*_{FI2}, Sm-C^*_{FI1}, and Sm-C^*_A phases are characterized by four- and three- and two-layer superlattices, respectively, while a periodicity incommensurate with the layer spacing was observed in Sm-C^*_α. A "clock" model assuming a constant increment $\Delta\Psi_j$ between adjacent layers and a corresponding helical Ψ_j arrangement agrees with our experimental observations. We note that extending our experimental technique to include polarization analysis of the diffracted beam should provide further insight into the molecular structure of the Sm-C^* variants. The tensorial character of the resonant scattering structure factor predicts different polarization states for the diffracted x-ray beam, depending on the model assumed for the molecular arrangements. In conclusion, the resonant scattering technique clearly shows great promise as a means of obtaining otherwise unavailable information about molecular arrangements in many unique phases of condensed matter.

We are grateful to H. Baltes and T. Lenhard for extensive technical assistance, and to I. Robinson, H. Baltes, T. Lubensky, and B. Pansu for stimulating and critical discussions. This work was supported in part by a National Science Foundation grant. One of us (P. M.) would like to acknowledge support from a NSF Fellowship. The NSLS is operated by Brookhaven National Laboratory under Contract DE-AC02-76CH00016 with the U.S. Department of Energy, Office of Basic Energy Sciences.

[1] A. D. L. Chandani *et al.*, Jpn. J. Appl. Phys. **28**, L1265 (1989).
[2] A. Fukuda *et al.*, J. Mater. Chem. **4**, 997 (1994).
[3] Y. Yamada *et al.*, Jpn. J. Appl. Phys. **29**, 1757 (1990).
[4] Y. Takanishi *et al.*, Jpn. J. Appl. Phys. **30**, 2023 (1991).
[5] Y. Takanishi *et al.*, Phys. Rev. E **51**, 400 (1995).
[6] P. Hamelin *et al.*, J. Phys. II (France) **3**, 681 (1993).
[7] H. T. Nguyen *et al.*, Liq. Cryst. **17**, 571 (1994).
[8] K. Ema *et al.*, Phys. Rev. E **47**, 1203 (1993).
[9] Y. Galerne and L. Liebert, Phys. Rev. Lett. **66**, 2891 (1991); Ch. Bahr and D. Fliegner, *ibid.* **70**, 1842 (1993).
[10] Careful optical and ellipsometry work was able to confirm a herringbonelike alternating orientation of molecules in Sm-C^*_A layers, with correspondingly antiparallel in-layer polarizations (Ref. [9]).
[11] T. Isozaki *et al.*, Jpn. J. Appl. Phys. **31**, 1435 (1992).
[12] K. Hiraoka *et al.*, Jpn. J. Appl. Phys. **30**, L1819 (1991).
[13] H. Orihari and Y. Ishibashi, Jpn. J. Appl. Phys. **29**, L115 (1990); B. Zeks and M. Cepic, Liq. Cryst. **14**, 445 (1993); V. L. Lorman, A. A. Bulbitch, and P. Toledano, Phys. Rev. E **49**, 1367 (1994).
[14] M. Cepic and B. Zeks, Mol. Cryst. Liq. Cryst. **263**, 61 (1995); V. L. Lorman, Mol. Cryst. Liq. Cryst. **262**, 437 (1995); A. Roy and N. Madhusudana, Europhys. Lett. **36**, 221 (1996).
[15] V. E. Dmitrienko, Acta Crystallogr. Sect. A **39**, 29 (1983).
[16] For an example of resonant x-ray diffraction applied to *crystalline* materials, see D. H. Templeton and L. K. Templeton, Acta Crystallogr. Sect. A **42**, 478 (1986).
[17] 10OTBBB1M7 racemate shows the following phase sequence: isotropic, Sm-A, Sm-C, Sm-C_A, and crystal phases.
[18] The two Ising models were originally proposed for temperature ("T") and electric field ("E") induced transitions. For $\nu > 3$, the Ising sequences are explicitly different, giving for $\nu = 4$ $\Delta\Psi_j = \pi, 0, \pi, 0$ (T Ising) versus $\Delta\Psi_j = \pi, 0, 0, \pi$ (E Ising). A fuller discussion, along with other examples of Ψ_j and $\Delta\Psi_j$ sequences for various ν is given in Ref. [2].
[19] A molecular form factor explanation (i.e., minimum in form factor at half-order peak position) for the intensity reduction between the quarter- and half-order peaks is unlikely, as the same intensity ratio is observed for all of the half-order peaks.
[20] This P_0 agrees well with a previously reported value. V. Laux, University of Lille I, Ph.D. thesis, 1997; V. Laux *et al.*, Liq. Cryst. (to be published).
[21] With our current resolution, we are also unable to resolve any distinct splitting features in the resonant peaks characteristic of the Sm-C^*_{FI1} and Sm-C^*_{FI2} phases. Absence of resolvable split peaks implies an optical pitch of greater than approximately 1 μm.